Controllers' robust design for PMSM drive fed with PWM voltage inverter with elastic joint and inertia load variation

Marcus Alexandre T. F. de Sousa, Stéphane Caux, Maurice Fadel

Controllers' robust design for PMSM drive fed with PWM voltage inverter with elastic joint and inertia load variation

Marcus Alexandre T. F. de Sousa, Stephane Caux, Maurice Fadel
Laboratoire d'Electrotechnique et d'lectronique Industrielle, LEEI-UMR-INPT-CNRS
2, rue Charles Camichel, BP 7122, 31071, Toulouse, France
(marcus, caux, fadel)@leei.enseeiht.fr

***Abstract*— A detailed design and comparisons of PID and LQ - State Space Controllers for Permanent Magnet Synchronous Machine (PMSM) loaded with elastic joint to a mass are presented. Step by step analyse for PID and LQ tuning is conduced for PMSM drive and varying load. A load inertia variation is taken into account to define the strategies used to calculate the optimum PID and LQ controllers that ensure the drive system stability and performance. Simulation results verify and compare the robustness of the controllers. Complexity of synthesis and performances obtained are discussed on an actual PMSM drive fed with a PWM voltage inverter controlled in current.**

I. Introduction

The Permanent Magnet Synchronous Motor (PMSM) is the most used drive in machine tool servos and modern speed control applications due to its desirable features (compact structure, high air-gap flux density, high power density, high torque to inertia ratio, and high torque capability). However, the control performance of the PMSM system is strongly influenced by the unpredictable plant parameters variation, external load disturbance and nonlinear dynamics [1] [2] [3]. For example, in machine tools operation, railway traction, and rolling mill drive the mechanical load varies considerably under certains operating conditions. Moreover, in many PMSM drive industrial applications the mechanical transfer elements (shafts, gears, friction, backlash, etc) introduce imperfections that must be considered in dynamic speed drives. The influence of inverter in such control is commonly neglected but an accurate current control and torque control contribute to the accurate position or velocity PMSM control. [4].

The aim of this paper is to propose a design method of speed closed-loop controllers for the PMSM-Elastic Load system (PMSMEL). The speed controllers under consideration are: a PID controller and a State Space Controller with integral action on the load speed error. To elaborate the controllers design strategies the load inertia variation is taken into account. In this paper a two-mass system is considered for mechanical part so, the PMSM and the load are connected through a shaft. The mechanical system dynamic characteristics with a large load inertia variation is presented in II. The PID synthesis is driven in frequency domain and state space corrector is studied by LQ optimisation in III.

Simulation results on the mechanical model show the performance robustness to load parameter variation characteristics of the proposed controllers. Detailed analyses through simulations comparing the performance between the controllers are given in IV. The complete controller performed is used in V, in a global set-up including PWM inverter switched current control in the LQ velocity closed-loop control.

II. Dynamic model of the system

The electrical machine model of a PMSM can be described in the rotor rotating reference frame as follows [5]:

$$\frac{di_d}{dt} = \frac{1}{L_d}(v_d + p\omega_m L_q i_q - R i_d) \quad (1)$$

$$\frac{di_q}{dt} = \frac{1}{L_q}(v_q - p\omega_m L_d i_d - R i_q - p\omega_m \psi_{dm}) \quad (2)$$

where v_d and v_q are d-q axis stator voltages, i_d and i_q are d-q axis stator currents, L_d and L_q are the d-q axis inductances, R is the stator winding resistance, ψ_{dm} is the flux linkage of the permanent magnets, ω_m is the angular velocity of the motor shaft and p is the number of pole pairs. The electromagnetic torque is stated as :

$$T_m = 3p[\psi_{dm} i_q + (L_d - L_q) i_d i_q]/2 \quad (3)$$

The basic principle in controlling a PMSM drive is based on field orientation. If $i_d = 0$ the electromagnetic torque T_m is then proportional to i_q, which is determined by closed-loop control. Since the PMSM is driven by a current-source inverter, i_q is a known quantity and thus serves as input to the motor. For velocity control purpose considering a smooth poles PMSM equation (3) can be reduced to :

$$T_m = k_t i_q \quad (4)$$

where $k_t = 3P\psi_{dm}/2$

Considering the mechanical system described by Fig. 1 the PMSM-Elastic Load system can be represented by the the speed control system block diagram shown in Fig. 2. The dynamic of PMSMEL in the nominal condition without

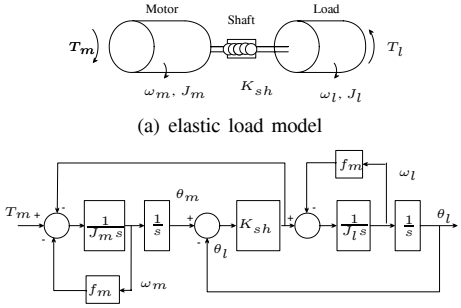

(a) elastic load model

(b) Block diagram

Fig. 1. Modeling of mechanical system

external load disturbances is given by:

$$\begin{aligned} J_m\omega_m s &= T_m - f_m\omega_m + T_{sh} && (5)\\ J_l\omega_l s &= -f_m\omega_l - T_{sh} && (6)\\ \theta_m s &= \omega_m && (7)\\ \theta_l s &= \omega_l && (8)\\ T_{sh} &= K_{sh}(\theta_l - \theta_m) && (9) \end{aligned}$$

where : s is the Laplace operator, J_m and J_l are the motor and load inertias respectively, θ_m and θ_l are the motor and load angular positions respectively, f_m is the viscous friction coefficient, T_{sh} is the shaft torque, ω_l is the load speed. In state space form the model (5)-(9) can be expressed as follows:

$$\begin{aligned} \dot{x} &= Ax + Bu \\ y &= Cx \end{aligned} \qquad (10)$$

where control input $u = T_m$, the state vector $x = [\omega_m\ \omega_l\ \theta_m\ \theta_l]^t$, output vector $y = w_l$, $C = [0\ 1\ 0\ 0]$, .

$$A = \begin{bmatrix} -\frac{f_m}{J_m} & 0 & -\frac{K_{sh}}{J_m} & \frac{K_{sh}}{J_m} \\ 0 & -\frac{f_m}{J_l} & \frac{K_{sh}}{J_l} & -\frac{K_{sh}}{J_l} \\ 1 & 0 & 0 & 0 \\ 0 & 1 & 0 & 0 \end{bmatrix} \quad B = \begin{bmatrix} \frac{1}{J_m} \\ 0 \\ 0 \\ 0 \end{bmatrix} \qquad (11)$$

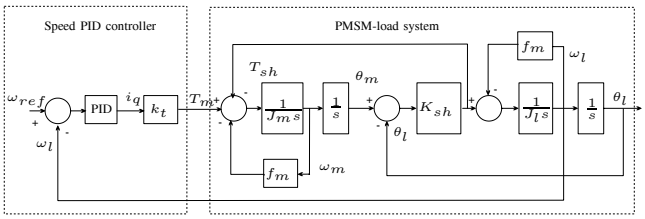

Fig. 2. The block diagram of speed control system of the PMSM-load system

The closed-loop transfer function $H(s)$ from motor torque T_m to load speed ω_l is given from (10) to obtain :

$$\frac{\omega_l(s)}{T_m(s)} = \frac{1}{2f_m\left[\frac{J_m J_l}{2f_m K_{sh}}s^3 + \frac{J_m f_m + f_m J_l}{2f_m K_{sh}}s^2 + \frac{J_t K_{sh} + f_m^2}{2f_m K_{sh}}s + 1\right]} \qquad (12)$$

where $J_t = J_m + J_l$

The natural resonant frequency ω_{np} and damping factor ζ_p are calculated from the poles of the transfer function $H(s)$:

$$\omega_{np} = \sqrt{\frac{J_t K_{sh}}{J_m J_l}} \quad , \quad \zeta_p \cong \frac{1}{4} f_m \sqrt{\frac{J_t}{J_m J_l K_{sh}}} \qquad (13)$$

Defining the bounds of load parameter variation J_l as follows:

$$J_l = [J_{l_{min}}\ J_{l_{max}}] \qquad (14)$$

Classical industrial limitations provide :

$$\begin{aligned} J_{l_{min}} &= J_{l_o}/2 \\ J_{l_{max}} &= 5.J_{l_o} \end{aligned} \qquad (15)$$

The Fig. 3 represents the bode diagram of the transfer function $H(s)$. With inertia variations the gain abruptly increases near the mechanical resonant frequency ω_{np}.

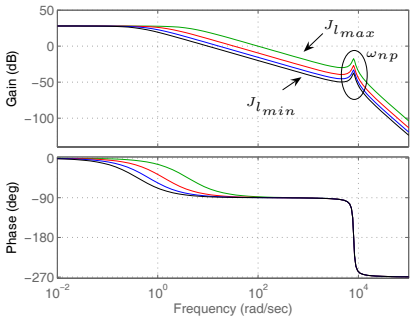

Fig. 3. The Bode diagram of the mechanical system with load parameter variation

III. PID AND LQ MODERN CONTROL DESIGNS

A. PID controller's Design

PID control based on the motor/load speed behavior is the most common controller structure used in industrial motor [6]. However, tuning of a PID controller requires knowledge of the nominal system's parameters (J_m, J_l, f_m, K_{sh}, etc). Due to the changes of the operating conditions or process/load disturbances, the dynamics of the system often change. If the conception of the closed loop control system takes into account only the information concerning the nominal system model, it might become unstable. For a robust control the uncertainties of the systems must be considered in the PID control design.

The PID controller shown in Fig. 2 has the following transfer function:

$$PID = K_p \cdot \left[1 + \frac{1}{s \cdot T_i} + \frac{s \cdot T_d}{1 + s \cdot aT_d}\right] \qquad (16)$$

The choice of the PID parameters (K_p, T_i, T_d, a), to obtain the desired response, is based upon the application requirements. The PID controller is designed in order to increase the system closed-loop bandwidth (e.g. higher velocity response) and to get a cross over frequency ω_c much lower than the mechanical natural frequency ω_{np}. The fact that the control input can not exceed the maximum motor torque must be

considered in the determination of the controller to not excite nonlinear phenomena.

It is well known that the proportion gain K_p is used to increase the systems bandwidth, as well as, the system bandwidth determines speed of response and it is limited by the dominant poles. The choice of the K_p gain or equivalently the crossover frequency ω_c must be a trade off between a fast enough motor/load response and a damped enough load behavior.

Considering a maximum tolerable overshoot of 5% of the load speed response as the main criterium to be satisfied with the PID. Moreover, a high rise and setting time response due to classical industrial applications requirements must be obtained.

Before calculating the optimum PID controller we are remaining that the motor parameters are known. The motor parameters are considered as unchangeable nominal values. Although the inertia load parameter will be characterized by the variation given by (15).

Taking into account the above informations, a strategy to determine the optimum PID controller for the system is defined. The strategy is developed as followed:

1) Three different load inertia references are studied :
   - load minimum inertia reference (1): $J_l = J_{l_{min}}$
   - load nominal inertia reference (2): $J_l = J_{l_o}$
   - load maximum inertia reference (3):$J_l = J_{l_{max}}$

   these three load inertia references give as consequence three nominal systems parameters value.

2) For each load inertia reference only Kp is tuned in the PID parameters. As result we have three sets of PID parameters:
   - set (1): K_{p_1}, T_{i_1}, T_{d_1}, a_1
   - set (2): K_{p_2}, T_{i_1}, T_{d_1}, a_1
   - set (3): K_{p_3}, T_{i_1}, T_{d_1}, a_1

   obviously : $K_{p_3} > K_{p_2} > K_{p_1}$.

3) For every set of the controller parameters, the overshoot evolution of load speed response is analysed while the load inertia is varying from $J_{l_{min}}$ to $J_{l_{max}}$. The overshoot evolution results are shown in Fig. 4.

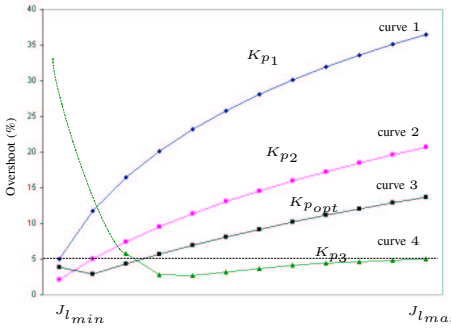

Fig. 4. The overshoot evolution of load speed response (the load inertia is varying from $J_{l_{min}}$ to $J_{l_{max}}$)

Curve 1 shown in Fig. 4 which depends on the first set of controller parameters, gives an overshoot exceeding the criterium of 5% while the load inertia parameter is increasing towards the maximum inertia value. Although the stability of the system is guarantied in all the load inertia range variation. The same situation appears for the curve 2, although the overshoot evolution is giving a more satisfying result. Observing curve 4, the criterium is respected in almost all of the inertia load variation range. The exception appears in the case where the load inertia approach the minimum value of the inertia range variation. At this moment the system becomes unstable (dashed line).
The three sets of parameters do not provide satisfying results, while the compromise between stability and the robustness criterium is not fulfilled.

4) To calculate the optimum PID parameters the two most satisfying sets of PID parameters are used as reference. This means that the optimum value $K_{p_{opt}}$ has to lie necessarily between K_{p_2} and K_{p_3}.

$$[K_{p_2}\ K_{p_{opt}}\ K_{p_3}] \tag{17}$$

Moving from the minimum value of the range K_{p_2} until the maximum value K_{p_3}, $K_{p_{opt}}$ is detected. $K_{p_{opt}}$ will be find in the point where the system is still marked by stability.

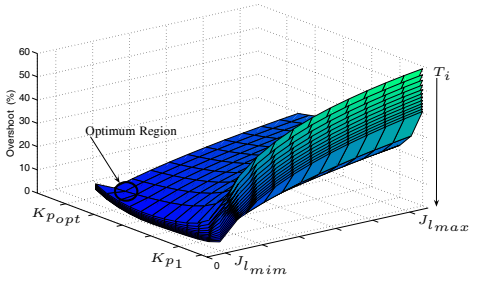

Fig. 5. The overshoot evolution of load speed response for K_p , J_l and T_i variation.

To verify the strategy, simulations of the closed-loop controller are conduced. In the simulated results, shown in Fig 5, K_p is changed from $K_{p_{min}}(K_{p_1})$ to $K_{p_{opt}}$. In each case, the load inertia is moving from $J_{l_{min}}$ to $J_{l_{max}}$. With the variation of these two parameters, the overshoot of the system response provides a surface. T_i parameter is also studied. The variation of this parameter is chosen in the way that the system stays stable. Each surface corresponds to a different value of T_i. The arrow in the picture points to the region where the overshoot is the lowest whatever the inertia is, which corresponds to $K_{p_{opt}}$. The reason why T_i parameter is included in this analyse, is to show that even T_i vary, the optimum region does not change.

B. State Space Controller

In this section a state space technique is used to assign closed-loop poles. State feedback gains are computed using LQ approach. An integration is commonly added to this classical scheme, the integral term K_i on the load speed error is needed to eliminate steady state errors if torque disturbances occur.

Considering that the dynamics of the system are given by:

$$\dot{\widetilde{x}} = \widetilde{A}\widetilde{x} + \widetilde{B}u \tag{18}$$

with, the state vector : $\widetilde{x} = [\omega_m \ \omega_l \ \theta_m \ \theta_l \ x_i]^t$ where x_i is the state of the integral term. The full state vector x is measured (or observed). The matrix $\widetilde{A}$ and $\widetilde{B}$ are respectively expressed as:

$$\widetilde{A} = \begin{bmatrix} A & \emptyset_{4*1} \\ -C & 0 \end{bmatrix} \ , \widetilde{B} = \begin{bmatrix} B \\ 0 \end{bmatrix}$$

with A and B the matrixes of the state space model given by (11). The vector of control input u is written as:

$$u = -K\widetilde{x} \tag{19}$$

with $K = [k_1 \ k_2 \ k_3 \ k_4 \ k_i]$. K is the the matrix gain of the state space law. The integral term k_i is computed also in matrix K so k_i is negative that explain sign (-) used in the block diagram of Fig. 6 representing the LQ controller.

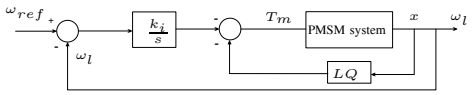

Fig. 6. The LQ regulator

Under state feedback $u = -K\widetilde{x}$, the closed-loop dynamics of the system are given by

$$\dot{\widetilde{x}} = [\widetilde{A} - \widetilde{B}K]\widetilde{x}$$

From (18), the quadratic cost function J_{LQ} and the control input u are given as follows:

$$J_{LQ} = \int_0^\infty (\widetilde{x}^t Q \widetilde{x} + u^t R u) dt \tag{20}$$

$$u = -K\widetilde{x} \tag{21}$$

with $R > 0$ et $Q \geq 0$.

The weighting matrixes Q and R to satisfy the control objectives of the system are given by:

$$Q = \begin{pmatrix} 0 & 0 & 0 & 0 & 0 \\ 0 & \alpha & 0 & 0 & 0 \\ 0 & 0 & 0 & 0 & 0 \\ 0 & 0 & 0 & 0 & 0 \\ 0 & 0 & 0 & 0 & \beta \end{pmatrix} \tag{22}$$

$$R = (\gamma) \tag{23}$$

where

α: weight for reference tracking performance,

β: weight for steady-state error management,

γ: weight for control input limitation,

The major problem of this control design is the selection of the weights in the quadratic cost function. The weight factors α, β and γ can be selected by trial and error method using off-line MATLAB simulation according to design specifications. For this purpose some importants characteristics about α, β and γ must be discussed:

- α imposes the contraints to the load speed dynamics. For high value of α the system response is slowing. The load speed overshoot is directly correlative with α.
- β gives the steady-state error dynamics. For high value of β the system response becomes fast (short rising time).
- γ is used to limit the maximum control input (motor torque) of the system. High values of γ results in high contraints of the maximum T_m. Therefore the settling and the rise time is increased.

To determine the optimum LQ weights the following strategy is developped:

1) The highest load inertia is used like reference.
   - load inertia reference : $J_l = J_{l_{max}}$

   The system parameter values are composed by the nominal motor parameters and load inertia.
2) Using the trial and error method and the knowledge of the weights characteristics, a set of LQ parameters is defined.
3) The system eigenvalues are analyzed when the load inertia is varying from $J_{l_{min}}$ to $J_{l_{max}}$.
4) If the robustness criterium, the maximum motor torque permitted, the condition of stability and the aim of high rise and settling time are achieved the optimum LQ weights are found. If not return to step 2.

The Fig. 7 shows the closed-loop poles of the PMSMEL with LQ control. The system becomes unstable ($\Re(s) > 0$) for $J_{l_{min}}$. The instability is due to the small weight fixed for control input ($\gamma = 0.001$), no contraints about T_m and β has a high value (fast dynamic). β is extremely important to determine the system stability or instability in the case where ($\gamma/\alpha > 100$, γ and $\alpha < 0$).

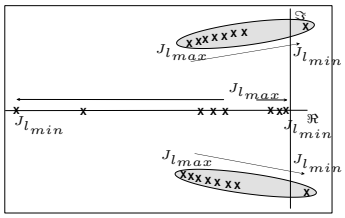

Fig. 7. Closed-loop control poles. $J_l = J_{l_{max}}$. $\alpha = 0.1$, $\beta = 500$ and $\gamma = 0.001$

Where the relation ($\alpha/\gamma > 100$, γ and $\alpha > 0$), the dominant closed-loop poles are placed near the real axis origin, system response is considerably slow. To accelerate the system response β has to be extremely high. The Fig. 8 shows the

closed-loop poles of the PMSMEL system for the α, β and γ optimum weight values achieved. The system is ever stable, and no overshoot is observed for every value of the load inertia.

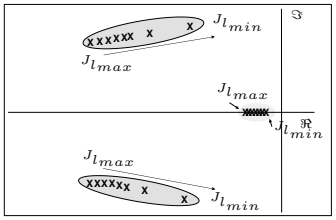

Fig. 8. Closed-loop control poles. $J_l = J_{l_{max}}$.

IV. Comparisons of the 2 controllers

To investigate the effectiveness of the two optimum proposed controllers, PMSMEL system simulation are conduced. The motor and load parameters are reported in Appendix.

The time response of the optimum PID controller system to a step in the load speed reference is shown in Fig 9.(a). The overshoot and settling time goes up when the load inertia augment. The criterium of robustness is not achieved (5% overshoot maximum). However, the closed-loop system is stable for every load inertia variation. The optimization only keep the stability but the system performances (response time, overshoot) vary.

Fig 9.(b) shows the system response with the LQ controller. The closed-loop system is ever stable and excellent performance of robustness is achieved. The dynamic response is easy controllable. The maximum control input effort necessary is 0.99Nm.

V. LQ controller on complete PMSM-EL drive

To verify the results obtained with the best LQ controller, a complete PMSMEL control experimental setup (Fig. 10) is simulated. The mechanical part is not the only element simulated but also the complete PWM inverter and its current control is implemented. The three-phase voltage source inverter (PWM Inverter) is composed by a set of 3x2 IGBTs with a carrier frequency of 20kHz. The maximum DC Source voltage available is 600 volts. To drive such device 3 duty cycles must be generated to obtain the ON/OFF switch orders. These states are obtained comparing 3 voltage references to a 20kHz symetric slop. The 3 references are computed through a 2 to 3 dimensional transformation. The Park transformation and the rotor position feedback is used to generate the dq-axis current (i_d, i_q). This transform allows to control 2 constant current value in a fixed frame rotating with the machine. Moreover, in this frame only the q axis current produces an effective torque so, a classical current control fixing $(i_d = 0)$ and $(i_q = Iref)$ is sufficient. The current control is achieved only by DC bus and 2 machine lines current measurements. The scheme is implemented with an anti-windup structure (Parameters in appendix).

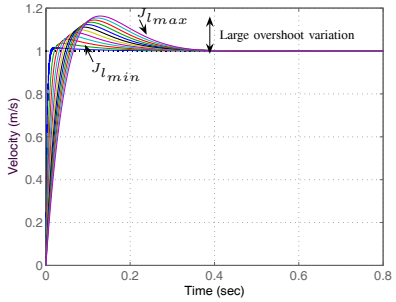

(a) PID step response

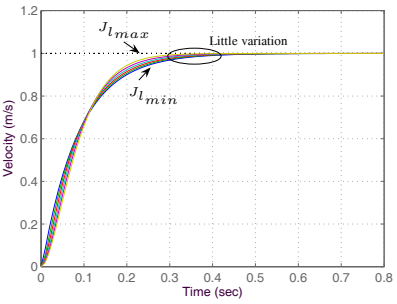

(b) load speed response LQ controller

Fig. 9. (a) Simulated load speed step response (optimum PID), with load inertia variation from $J_{l_{mim}}$ to $J_{l_{max}}$. Effective robustness on stability, but variation in transient phase. (b) Simulated load speed step response (optimum LQ controller), with load inertia variation from $J_{l_{mim}}$ to $J_{l_{max}}$. Effective performance robustness and system stability.

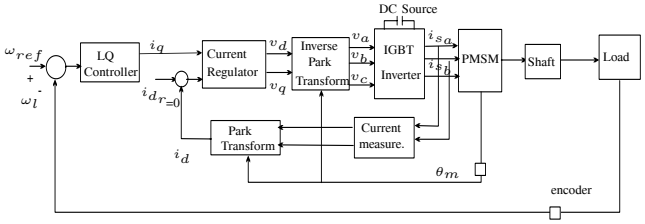

Fig. 10. The schematic diagram of the PMSMEL control experimental setup.

The Fig. 11 shows the load speed response for a load speed reference equal to 100 rpm. The results obtained is very close to the results shown in Fig. 9. A zoom at steady state shows the effective control of the velocity but the inertia variation allows the current (the torque) to vary in different manner during each sampling period. The less the inertia is the greater the speed variation is in a period (1/20k s). But the control scheme and the sampling period is sufficient to be accurate.

A more complex velocity reference to follow has been generated. It consist in an acceleration slop a fixed velocity +100rpm constant phase, decreasing to -100rpm and return to 0rpm. In all of the load inertia range variation the controller performance is satisfied.

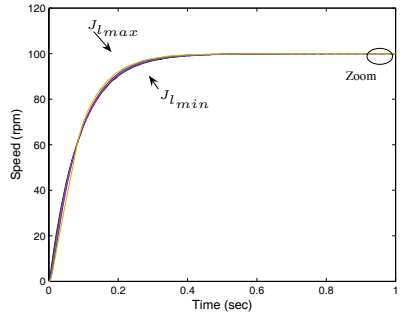

(a) load speed response

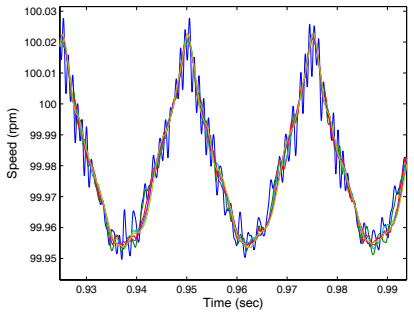

(b) Zoom

Fig. 11. (a) Simulated load speed response of a PMSMEL control experimental setup ($\omega_{ref} = 100\ rpm$), with load inertia variation from $J_{l_{mim}}$ to $J_{l_{max}}$. In (b) a little load variation is observed.

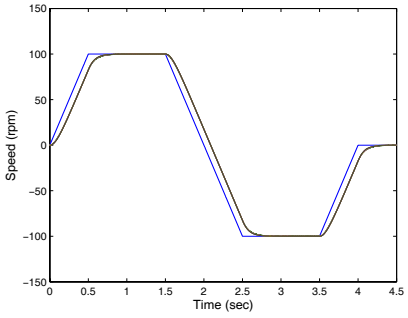

Fig. 12. Simulated load speed response, with load inertia variation from $J_{l_{mim}}$ to $J_{l_{max}}$. The speed reference consists of a increasing and decreasing ramp reference. Good performance is achieved.

VI. Conclusion

This paper describes the robust design and comparaison of classical controllers in PMSM drive in application of elastic load with large load inertia variations.

Classical synthesis of a PID in frequency domain is not robust but an optimisation can be made to remain stable whatever the inertia is (in presence of limited variations). State Space Controller allows accurate pole placement, but actual torque limitation must be considered to have both transient and permanent controlled desired behavior. LQ synthesis allows to fix performances and to limit torque magnitude in the same way. LQ synthesis is difficult due to gains acting directly on outputs performances and input limitation. Testing different coefficients allows to extract the optimal LQ regulator that let the system in stable region and around fixed performances. A robust design of the standard controllers adapted to the load and inertia variation guaranties the system stability and performance robustness.

VII. Appendix

The system parameters used in the simulation.

$R = 10.7\ ohm$	$K_t = 0,8\ N.m/A$
$L = 7,4\ mH$	$f_m = 20.10^{-3}\ N.m.s/rad$
$p = 4$	$K_{sh} = 1740\ N.m/rad$
$J_m = 0,027.10^{-3}\ Kg.m^2$	$\omega_{np} = 8033,14\ rad/s$
$J_{l_o} = 20.10^{-3}\ Kg.m^2$	

PI current control

$K_p = 100$	$T_i = 0,1$

LQ parameters.

$\alpha = 0.1$	$\beta = 500$	$\gamma = 0.001$

References

[1] J. K. Ji and S. K. Sul, *Kalman Filter and LQ Based Speed Controller for Torsional Vibration Suppression in a 2-Mass Motor Drive System*, IEEE Transaction on Industrial Electronics, vol. 42, no.6, December 1995.

[2] D. J. Shin and U. Y. Huh, *Robust Motion Controller Design for Servo System with 2 Mass Characterisics*, Proceedings of 6th International Workshop on Advances Motion Control, AMC 2000, Nagoya, Japan, 2000, pp. 423-426.

[3] Y. R. Chen, N. C. Cheung and J. Wu, *H_∞ Robust Control of Permanent Magnet Linear Synchronous Motor in High-Performance Motion System with Large Parametric uncertatinty*, Proceedings of the Power Electronics Specialists Conference, PESC 02, June 23-27, 2002, pp.535-539.

[4] S. Moberg and J. Öhr, *Robust Control of a Flexible Manipulator Arm: A Benchmark Problem*, Proceedings of 16th World Congress of the International Federation of Automatic Control (IFAC) , Prague, Czech Republic, July 3-8, 2005.

[5] T. L. Hsien, M. C. Tsai and Y.Y. Sun, *H_∞ Robust Speed Control of Permanent Magnet Synchronous motors: Design and Experiments*, Proceedings of the 1996 IEEE IECON 22nd International Conference on, August 5-10, 1996, vol. 2, pp.1177-1182.

[6] G. Ferretti, G. Magnani and P. Rocco, *Load Behavior Concerned PID Control for Two-Mass Servo Systems*, Proceedings of the 2003 IEEE/ASME International Conference on Advanced Intelligent Mechatronics (AIM 2003), Port Island, Japan, vol. 2, pp. 821-826.

[7] L. Peyras, S. Caux and M. Fadel, *Robust Observer for sensorless Control of Synchronous Drive with Uncertain Parameters*, Proceedings of EPE 2003, 1Oth European Conference on Power Electronics ans Applications, Toulouse, France, Sept 2-4, 2003.